Journal of Advanced Research in Fluid Mechanics and Thermal Sciences

Journal homepage:
https://semarakilmu.com.my/journals/index.php/fluid_mechanics_thermal_sciences/index
ISSN: 2289-7879

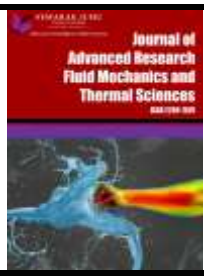

Model of Selectivity of Membrane Processes and Dissolution of Impurities in a Membrane Pore in a Medium with Surface-Active Micelles

Marat Satayev[1,2,*], Abdugani Azimov[1,2], Arnold Brener[2], Nina Alekseeva[1], Zulfia Shakiryanova[1]

[1] LLP InnovTechProduct, Industrial Zone Ontustik, 160012, Shymkent, Republic of Kazakhstan
[2] M. Auezov South Kazakhstan University, 160011, Shymkent, Republic of Kazakhstan

ARTICLE INFO

Article history:
Received 13 April 2024
Received in revised form 15 July 2024
Accepted 26 July 2024
Available online 15 August 2024

Keywords:
Model; selectivity; membrane; pore; surface-active micelles

ABSTRACT

It is shown that concentration polarization affects the size of the Knudsen layer and the mechanism of mass transfer in the Knudsen layer is established. Based on the analysis of the selectivity patterns of ultrafiltration membranes, an equation was obtained for calculating the total probability of particle drift through the boundary diffusion layer and penetration into the Knudsen layer region and an equation for calculating the diffusion coefficient determined by the value of the derivative of the chemical potential in concentration. An equation is derived for determining the flow of particles to the membrane surface in the Knudsen layer by its thickness using the free path length of particles, the average velocity of thermal motion of molecules, the average residence time of particles in the Knudsen layer. The probability of particles passing through the pore is estimated, taking into account the influence of the activation energy for the passage of the solvent and the ratio of the interparticle distance in the pore to the free path length, and the selectivity of the membrane is estimated. An equation is obtained for calculating the length of the dissolution front in a micellar solution inside a membrane pore. An equation is obtained for calculating the kinetic factor in a micellar solution inside a membrane pore, taking into account the mass transfer coefficient along the interface, the diffusion coefficient, as well as the concentration of micelles in the medium and the solubilization rate constant. An effective design of a membrane apparatus for water purification is proposed.

1. Introduction

Membrane technology is attracting increasing attention in the field of separation due to its high efficiency, energy conservation, environmental protection and other advantages [1]. However, in the relevant theories of mass transfer, especially in limited conditions, there is a lack of understanding of the general mechanisms of mass transfer and control methods, which seriously limits the design and development of appropriate membrane materials. The mechanism of limited mass transfer, influencing factors, manufacturing methods and types of preparatory materials are briefly described. Membrane technology is known as a cheaper alternative approach to produce high purity substances

* *Corresponding author.*
E-mail address: maratsatayev@mail.ru

https://doi.org/10.37934/arfmts.120.1.151175

[2]. The article discusses the state of advanced ceramic-based membranes in the field of oxygen separation at high temperature, including emerging issues related to selectivity and membrane separation. Kumar and Suneetha [3] analyzed the effect of diffusion on heat and mass transfer inherent in thermally radiating Williamson nanofluid over a stretchable surface through a porous medium under a convective boundary condition in the presence of thermal radiation and a chemical reaction. The coefficients of Brownian diffusion and thermophoresis are also taken into account.

Membrane technology is gradually being used as an alternative to the traditional separation and purification method in various industries [4]. Important performance indicators such as penetrant flow and rejection are closely related to fluid dynamics, mass transfer, and solutes. The relationship between concentration polarization and hydrodynamics in various configurations is discussed. The influence of process variables on the membrane characteristics and the interaction of the solute with the solvent membrane is also considered. According to Abubakar and Ahmad [5], the characteristics of membrane pores were determined by the multipoint BET method. The microstructure of locally produced baked clay from Nigeria was recorded using FESEM. Membranes made of clay were used to treat wastewater from the tannery. Polysulfone is a widely used material for ultrafiltration membranes, which has outstanding mechanical properties, high chemical resistance, good thermal stability and a wide operating pH range [6]. Mixing with hydrophilic material as additives such as cellulose has been intensively studied to improve membrane hydrophilicity. An attempt was made to develop a modified nanocomposite membrane made of graphene oxide as a potential adsorbent for the removal of lead ions by continuous adsorption [7]. The effect of the dynamic adsorption process was investigated together with the effect of flow rate, initial lead concentration and layer height. In the article by Lounder *et al.,* [8], membranes are manufactured by UV treatment of amphiphilic copolymers with a high content of zwitterion with the possibility of crosslinking to stabilize selective membrane layers, prevent excessive swelling and dissolution of copolymers. The mass fraction of zwitterion allows you to adjust the characteristics of the membrane, while the effective pore size and permeability increase with increasing content of zwitterion. Membranes have limited viability and suffer from instability and swelling due to their hydrophilic nature [9]. In this work, the permeability and rejection characteristics of multilayer membranes were improved by functionalization with ethylenediamine and polyethylene amine. Polyamide membranes manufactured by the method of interfacial polymerization with the participation of surfactants have demonstrated the potential of excellent membrane characteristics [10]. The presence of surfactants accelerates the diffusion of amine into the organic phase, causing a more complete reaction. In the study by Satayev *et al.,* [11], a mathematical model was developed for the dependence of the internal diffusion coefficient and hydrodynamic resistance on the structure and shape of the pores of a polymer membrane. In the article by Luo *et al.,* [12], for the first time it was reported about the creation of a selective membrane layer against the deposition of dyes based on a stable boroxine mesh. The pore size of the selective layer can be adjusted by changing reaction conditions such as concentration, temperature and degree of dilution. In the study by Gowda *et al.,* [13], the ability of the tested cells to create defects on the membrane surface through contact zones was recognized for the first time. It is proposed to modify the design of the tested cell, which reduce the contact zones, thereby potentially preserving the selectivity of the membrane.

Membrane ultrafiltration has become increasingly important as a simple and convenient process for concentrating, purifying and fractionating solutions of medium and high molecular weight solutes, and colloids, as well as for purifying water and other solvents containing solutes [14]. The emergence of this new method of molecular separation for both laboratory and industrial applications is almost entirely due to the development of a family of polymer membranes of a unique structure that demonstrate extremely high hydraulic permeability combined with the ability to retain

even fairly small molecules of solutes. A large number of processes associated with the transfer of heat or mass between a solid and a liquid are characterized by a thin boundary layer near the wall [15]. The boundary layer has a significant resistance to heat and mass transfer and is often a speed limiting factor. Any attempt to reduce the thickness of the boundary layer, for example, working in turbulent flow conditions, will improve the transfer rate. Another way to improve performance is to remove the boundary layer using an ultrafiltration boundary layer removal device.

Models of mass transfer through membranes are divided into those in which the membrane is the main transport resistance, and others in which additional resistances are formed by boundary layers of concentration and layers of particles [16]. In this work, researchers mainly use porous membranes, for which a model for mass transfer controlled by a membrane has been developed. Concentration boundary layers can be formed if permeable components are diffusionally transported along a gradient from the bulk concentration to the wall concentration, or if impermeable components are concentrated on the membrane surface. By establishing a mass flow balance around the differential cross-section of the membrane (membrane element), equations describing the removal rates of solvents and dissolved or dispersed molecules and their dependence on geometric and operating parameters are derived. The article by Espinoza-Gómez *et al.,* [17] presents a method for determining pore diameters and efficient transport through membranes using a mixture of oligosaccharides. The results are compared with the Maxwell–Stefan equations. The solute distribution coefficients are a function of the pore diameter according to the Ferry equation. Thus, with the pore diameter as the only unknown parameter, the rejection is described and the pore diameter is obtained using the Marquardt–Levenberg optimization procedure. The study by Aimar *et al.,* [18] suggests various aspects that need to be considered in order to understand and analyze the contamination and concentration polarization of porous membranes. In the first part, the properties of liquids and membranes are described and the orders of magnitude of flows and forces are given. Then the transfer phenomena and interactions that play a role in the mechanisms at the liquid/membrane interface are listed. Then the modeling of these various phenomena is considered, which allows us to offer a comparison between different restriction mechanisms. Fedosov *et al.,* [19] proposed a mathematical model for separating liquids containing acrylic dispersions and returning expensive technological components dissolved in them to the production cycle. The main limiting factor is the formation of a sediment layer on the membrane surface. This process is not stationary, since the thickness of the sediment layer varies both during the separation process and depending on the length of the membrane module. The influence of the sediment layer on the hydrodynamics and efficiency of mass transfer, its productivity and the quality of cleaning is determined. The calculation of the sediment layer and its effect on the separation process is performed using the microprocess method. This method is based on the balance of materials and energy and takes into account the viscosity and diffusion coefficients, which vary depending on the temperature and composition of the mixture. The dependences of the sediment thickness on the time and length of the membrane module and the selectivity coefficients on the concentration of the colloidal solution were obtained to determine the effective parameters of the baromembrane installation.

To achieve a certain separation using a membrane process, the first step is to develop a suitable membrane [20]. However, during the actual separation, for example, a pressure-controlled process, the characteristics of the membrane (or, better, the performance of the system) can vary greatly over time, and a typical behavior over time can often be observed: the flow through the membrane decreases over time. This behavior is mainly due to concentration polarization and clogging. The concentration polarization coefficient is a measure of the degree of concentration polarization in a membrane separation system [21]. In general, the concentration polarization coefficient shows the degree of loss of the driving force of penetration in relation to the total driving force between the

volumes of the liquid phase on the supply side and on the penetration side. Respectively, scientists have investigated and schematically presented the drops of the driving force along the direction of penetration in the case of hydrogen penetration through the membranes, as well as the cases of direct and reverse penetration. Bryll and Ślęzak [22] investigated the membrane transport of aqueous solutions without electrolytes in a single-membrane system with a membrane installed horizontally. The aim of the study is to analyze the influence of volumetric flows on the formation of concentration boundary layers. A mathematical model is presented for calculating the dependences of the concentration polarization coefficient (ζ_s) on the volumetric flow (J_{vm}), osmotic force ($\Delta\pi$) and hydrostatic force (ΔP) of various values. The property $\zeta_s = f(J_{vm})$ for $J_{vm} > 0$ and for $J_{vm} \approx 0$ and the property $\zeta_s = f(\Delta C_1)$ are calculated. In addition, the results of the simultaneous influence of ΔP and $\Delta\pi$ on the value of the coefficient ζ_s when $J_{vm} = 0$ and $J_{vm} \approx 0$ are investigated, and a graphical representation of the dependencies obtained during the study is presented. Mathematical dependences between the coefficient ζ_s and the Rayleigh number of concentration (R_C), providing an appropriate graphical representation, were also studied. In experimental testing, aqueous solutions of glucose and ethanol were used. According to Dmitriev and Kuznetsova [23], the applicability of the electrodiffusion method to the determination of mass transfer coefficients in the channels of flat-chamber membrane installations is discussed. Experimental and theoretical results are compared. Both similarities and differences between the equations describing processes on permeable and impermeable surfaces are noted. The conditions for the applicability of the electrodiffusion method to the modeling of reverse osmosis and ultrafiltration in flat channels of membrane installations are established. A discrete multilayer model of the deposition of solutes inside the pores of the membrane during ultrafiltration is proposed [24]. The model takes into account the time-dependent steric exclusion of solutes at the entrance to the pore and the difference between the deposition coefficients for the first and higher layers caused by the action of two-layer electrostatic repulsion forces between suspended and precipitated solutes. The defining differential equations are solved numerically for 2- and 3-layer deposition on the pore wall. In addition, a much simpler approximate solution with an error of less than 10% for the main practical scenario was obtained by the generalized averaging method for variable parameters. The curves of the compromise between permeability and selectivity for a single-layer coating (Langmuir adsorption), two-layer and three-layer cases at different values of the deposition coefficient from the upper to the first layer and the initial pore radius are calculated and compared. It is shown that the value of the deposition coefficient for higher layers of precipitated solutes can significantly affect the performance of the membrane. For the case of a single-layer coating, simple algebraic equations are derived to find the rejection coefficient and its minimum. They imply that the rejection coefficient can follow three scenarios: monotonically decreasing, monotonically increasing, or having a minimum. It is proposed to use a set of derived equations to determine the initial, minimum and steady-state values of the rejection coefficient and permeate flow along with the experimental selectivity-permeability compromise curve to find unknown physico-chemical and geometric parameters necessary to describe the ultrafiltration process of interest, optimize its technological parameters and change the membrane manufacturing process in order to obtain a more efficient membrane. In the article by Yi *et al.,* [25], an ultrafiltration cup with a dead end was continuously used to study the mechanisms underlying membrane fouling caused by a gel layer. Anionic polyacrylamide was used as a model contaminant for the gelation process in various ultrafiltration processes using two types of ultrafiltration membranes, for example, polyvinylidene fluoride (PVDF) (OM) membranes and TiO_2/Al_2O_3-PVDF membranes (MM); then a gelation model was created and systematically evaluated. The results show that the gelation process during ultrafiltration can be divided into three stages: “slow-fast-slow” flow attenuation curve. The value of the R^2 simulation curve still exceeded 0.90 for

both ohms and MM. Based on current knowledge, the proposed mechanism of gel layer formation and the mathematical model were feasible. According to Baikov and Bil'Dyukevich [26], a semi-integral method for determining the polarization of ultrafiltration is proposed and the specific features of the latter in laminar ultrafiltration in a flat channel are discussed. Diffusion in porous solids can take place by one of three mechanisms or by several of them at once [27]. These mechanisms are as follows: ordinary ("volumetric"), Knudsen and surface diffusion. In the absence of surface diffusion, the location of porous walls is not significant if the pores are large relative to the mean free path of the molecules, and the process is similar to conventional molecular diffusion contained in the pores. Knudsen diffusion occurs in pores, with small pore sizes. The effect of temperature and solvent on the structure and permeability of membranes limited, for example, by fluctuation bonds with limited degrees of freedom of volume was investigated by Pandey *et al.,* [28] using Monte Carlo simulation. The model in the study by Liu *et al.,* [29] proposed by Cohen is used to describe the diffusion process through polymer membranes subjected to externally applied tensile loads. This approach, based on the theory of continuum mechanics, is compared with a model developed using mesoscopic theory.

The purpose of the research by Mohammadi *et al.,* [30] was to obtain information for further development of a model of the ultrafiltration process. The process of formation of deposits on membranes during the treatment of wastewater containing emulsions and suspensions was studied, model wastewater included emulsions formed with the use of oil and gelatin. Therefore, modeling of diffusion processes in such membranes should rely more on the principles of molecular dynamics and generalized Maxwell-Stefan relations [31]. The framework of the mesoscopic approach, when strictly applied, requires the use of stochastic integral differential equations taking into account nonequilibrium statistical mechanisms. These equations are obtained in the limit of infinitely long-range order for intermolecular forces. However, studies by Snyder *et al.,* [32] and Horntrop *et al.,* [33], as well as numerical experiments with models of relaxation transfer nuclei and detailed computer modeling have shown that the mesoscopic approach can be extended to the short-range order of action of intermolecular forces. A method has been developed by Geraldes and De Pinho [34] for determining the mass transfer coefficient based on a change in the regeneration rate for membranes with a large surface area and high regeneration rates. The method was used to measure the mass transfer coefficients for the spiral module during nanofiltration. The aim of the work by Cherevko *et al.,* [35] was to describe diffusion in a membrane system associated with reversible chemical reactions in physical terms. Chemical reactions were modeled as intermolecular interactions. Thermodynamics of irreversible processes has been used to analyze all processes. The analysis of problems of diffusion through membranes, including a realistic boundary condition of the flow, is presented [36]. Membrane analysis is applied in the case of operations involving geomembranes.

The analysis of experimental and theoretical material on membrane processes has shown that the process of penetration of matter into the pores of membranes can be divided into several stages characterized by different probabilistic estimates. The substance enters from the depth of the continuous medium into the boundary diffusion layer, which is identified as diffusion transfer. The substance penetrates to the membrane surface through the Knudsen layer with a thickness of the order of the free path of molecules. In the Knudsen layer, the laws of diffusion transfer are not valid. The substance penetrates into the "entrance" of the pores on the surface of the membrane and diffuses inside the pores. The results obtained in this direction are preliminary. However, it is the constructive optimization of membrane apparatuses that promotes membrane regeneration, increases the productivity of the membrane apparatus and the efficiency of concentration of solutions that determines the intensity of mass transfer in membrane processes. Taking into account

the influence of parameters characterized by the value of the Knudsen layer, the full probability of particle drift through the boundary diffusion layer and the diffusion coefficient determined by the value of the derivative of the chemical potential in concentration, the free path length of particles, the average speed of thermal motion of molecules, the influence of the activation energy for the passage of the solvent, the length of the dissolution front in the micellar solution inside the membrane pore are necessary when modeling processes and devices, calculation and design of membrane equipment.

2. Methodology

In order to study the ultrafiltration treatment of water, we used the ultrafiltration unit shown in Figure 1.

The membrane apparatus consists of a rectangular body 0.7 m long, 0.25 m wide, 0.2 m high. The main part of the membrane apparatus is a membrane block made of 6 parallel rectangular membrane elements, between which parallel flow channels of $1.5\text{-}10^{-3}$m are formed, oriented from the inlet pipe of the separated mixture to the outlet pipe of the concentrate, the membrane elements consist of ribbed plates, porous substrates and semipermeable membranes, and the edges of both surfaces of the plate are arranged crosswise relative to each other at an angle of 145°.

Knowledge of the membrane structure is of great importance in solving the problems of developing a quantitative theory of membrane processes and their successful implementation.

The method by Dytnersky [37] was used to estimate the total porosity. The membrane sample, pre-weighed, is saturated with a wetting liquid and re-weighed, after which it is calculated ε_o

$$\varepsilon_o = \frac{G'_{об} - G_{об}}{V_м \rho_{ж}}, \tag{1}$$

The pore radius was determined by the flow rate of the liquid forced through the membrane. Measure the volume V_p liquid passing through the membrane during τ at a known constant pressure drop on the membrane, after which r is calculated using the Poiseuille equation

$$r = \sqrt{\frac{8\mu q l}{S_o f_o \Delta P}}, \tag{2}$$

The area S of the membrane surface required for the filtration process is determined by the formula

$$S=1{,}5\ (V/v)s, \tag{3}$$

Concentration polarization is determined by the formula [38]

$$\text{CP} = \frac{\exp\left(\frac{G_1}{\beta}\right)}{\varphi_И + (1-\varphi_И)\exp\frac{G_1}{\beta}}, \tag{4}$$

Considering that true selectivity $\varphi_u = 1$, get

$$CP = \exp\frac{G_1}{\beta}, \quad (5)$$

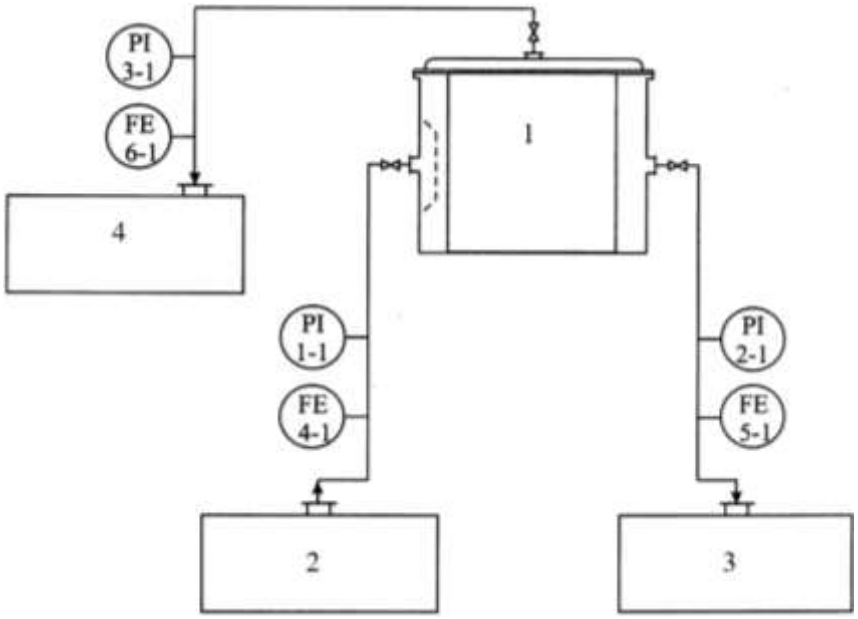

Fig. 1. Experimental installation for water purification to produce steam. 1 – membrane apparatus; 2 – container for the initial aqueous solution; 3 – container for purified water; 4 – container for permeate

The conducted studies of mass transfer for flat membrane channels allowed us to obtain the following equations for determining the mass transfer coefficient [39]

$$Sh = 0{,}023\, Re^{0,8}\, Sc^{1/3}, \quad (6)$$

where

$$Re = \frac{wd_э}{v}; \quad Sc = \frac{U}{D}; \quad Sh = \frac{\beta d_э}{D} \quad (7)$$

The average velocity of the flow through the channels slit - shaped in cross - section was determined by the formula given in the work [40]

$$V = 8{,}1 \cdot 10^3 \lambda W_0 \alpha^2 \Delta P \beta^2 \frac{1}{\eta l}, \quad (8)$$

To intensify the process of purification of aqueous solutions by ultrafiltration, we have proposed a more advanced design of the membrane apparatus, which allows to increase the productivity of the apparatus and the efficiency of separation of the mixture, eliminate stagnant zones, simplify the design of the apparatus by reducing the influence of concentration polarization [41]. One of the designs that meets the above requirements is a membrane apparatus developed by us with fixed membrane elements [41].

Figure 2 schematically shows the proposed apparatus, a longitudinal section; Figure 3 – section A-A; Figure 4 – ribbed surfaces of the membrane element plate.

The problem is solved by the fact that in a membrane apparatus containing a housing with the inlet pipes of the separated mixture and the concentrate outlet located on its opposite walls, a lid with a permeate outlet pipe, a membrane block made of parallel rectangular membrane elements, between which parallel flow channels are formed, oriented from the inlet pipe of the separated mixture to the outlet pipe of the concentrate, membrane elements consist of ribbed plates, porous substrates and semipermeable membranes, moreover, the edges of both surfaces of the plate are arranged crosswise relative to each other at an angle of 140-150^{o}.

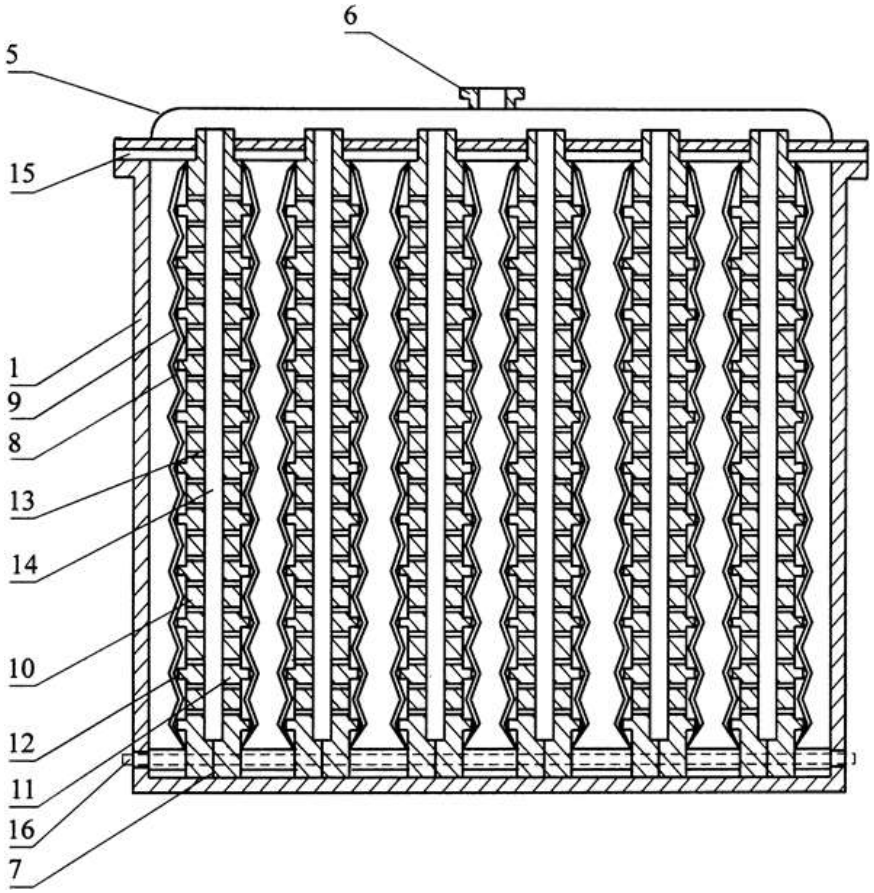

Fig. 2. Membrane apparatus with fixed membrane elements. 1 – housing; 2 – pipe for the input of the separated mixture; 3 - pipe for the output of concentrate; 4 - membrane block; 5 – lid; 6 - pipe for the output of permeate; 7 – plates; 8 - porous substrates; 9 – membranes; 10 and 11 - left and right parts of the plate; 12 – ribs; 13 and 14 - channels for the output of permeate; 15 – gasket; 16 - guide rod; 17 - diffuser

The membrane apparatus consists of a rectangular housing 1 with a nozzle 2 for the input of the separated mixture, a nozzle 3 for the output of the concentrate, a membrane unit 4. The housing 1 is closed with a lid 5 with a nozzle 6 for the output of permeate. The membrane element consists of a plate 7, porous substrates 8 and membranes 9. The plate 7 consists of a left 10 and right 11 parts with ribs 12, channels 13 and 14 for the output of permeate. Housing 1, membrane block 4, cover 5 is bolted through gasket 15. The lower part of the membrane block is fastened with a guide rod 16. A diffuser 17 is installed in the housing 1 opposite the inlet pipe 2.

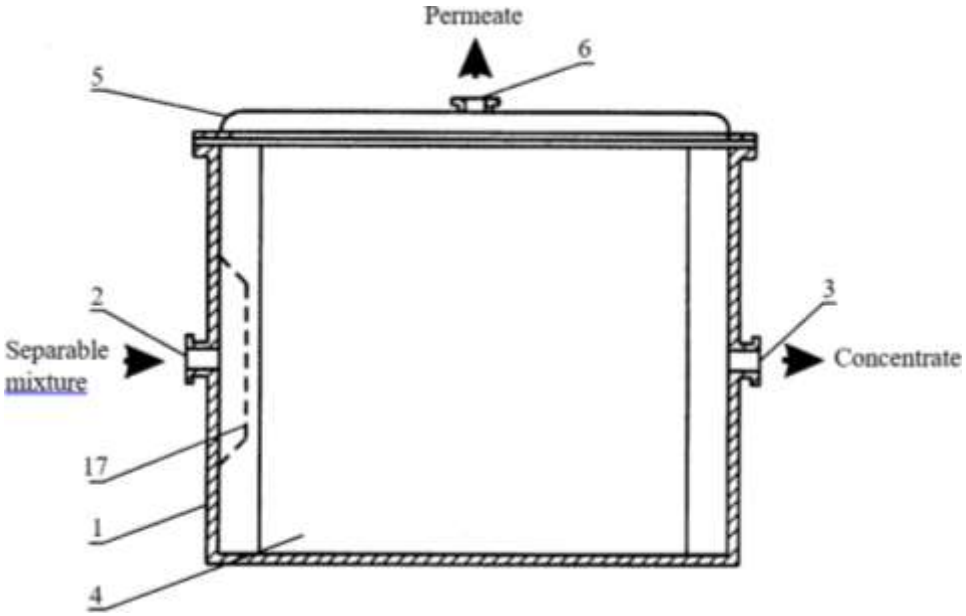

Fig. 3. Membrane apparatus in section A-A

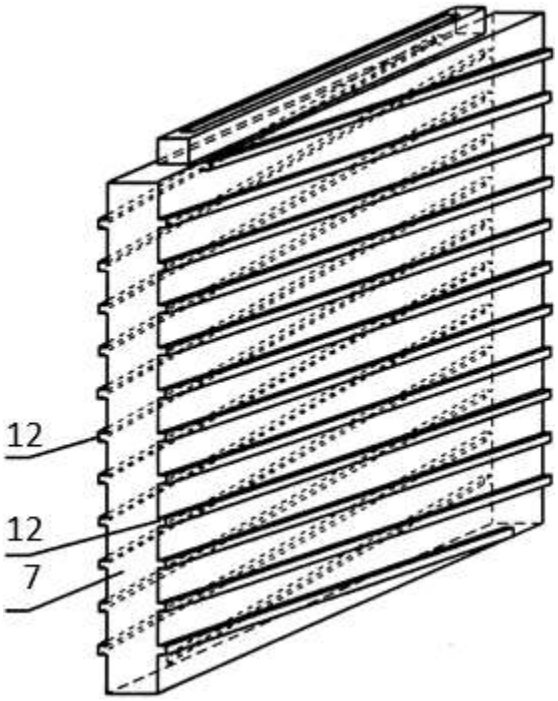

Fig. 4. Ribbed surface of the membrane element plate

The membrane apparatus works as follows.

The separated mixture through the nozzle 2, located in the housing 1, enters the membrane block 4 through the diffuser 17, the lower part of which is fastened with a guide rod 16 and is directed into the space between the membrane elements. Moving along the membranes 9 between the ribs 12, the mixture under pressure passes through the membranes 9, porous substrates 8 and through the channels 13 and 14 of the plate 7 is removed under the lid 5 and directed through the nozzle 6 to bring the permeate out. The concentrate is removed from the device through the nozzle 3. When the separated mixture passes between the inclined edges 12 of the plate 7, due to the fact that the edges of the surfaces of the plates 10 and 11 are arranged crosswise relative to each other at an angle of

140-150°, the resulting flows intersect and turbulate. The occurrence of turbulence of flows provides a decrease in the level of concentration polarization and an increase in the productivity of the membrane apparatus and the efficiency of concentration of solutions.

3. Results

3.1 Model of Selectivity of Membrane Processes and Dissolution of Impurities in a Membrane Pore in a Medium with Surface-Active Micelles

3.1.1 Probabilistic model of selectivity of membrane processes

The calculation of the selectivity characteristics of membrane separation of mixtures, based on the basic physico-chemical characteristics of the solution, permeate and retant, is a difficult task due to a large number of influencing factors [37]. In a study by Smirnov and Bartov [42], a probabilistic approach was effectively used to solve this problem. At the same time, estimates of the selectivity of nanofiltration membranes for individual ions were obtained. In this paper, we use a probabilistic approach to theoretically evaluate the selectivity of ultrafiltration membranes, in which the mechanism of the separation process differs significantly from the mechanism of separation in nanomembranes.

The process of penetration of a substance into the pores of ultrafiltration membranes can be divided into several stages characterized by different probabilistic estimates (Figure 5).

Firstly, the substance enters from the depth of the continuous medium into the boundary diffusion layer. This stage is identified as diffusion transfer.

Secondly, the substance penetrates to the membrane surface through the Knudsen layer with a thickness of the order of the free path of molecules. In the Knudsen layer, the laws of diffusion transfer are not valid. Thirdly, the substance penetrates into the "exit" of the pores on the surface of the membrane. And finally, fourthly, the substance diffuses inside the pores.

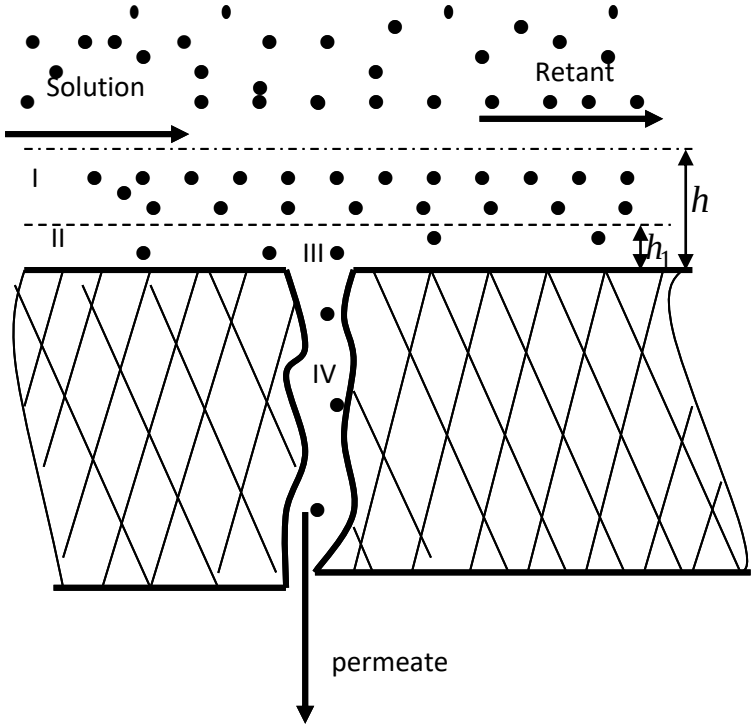

Fig. 5. Diagram of the membrane separation process

For each of these stages, their own estimates of the probability of penetration of particles of the separated solution are performed.

Zone I.

In the diffusion boundary layer, to estimate the probability of a particle drifting over a distance over time, we use the formula of the probability density of Brownian motion

$$P_1(s,\tau)=\frac{1}{\sqrt{4\pi D\tau}}\exp\left(-\frac{s^2}{4D\tau}\right), \tag{9}$$

Integrating the probability density of the Brownian walk over the residence time of particles in the diffusion boundary layer θ, we obtain an estimate of the average density of the probability distribution of drift in the diffusion boundary layer

$$P_{1s}(s)=\frac{1}{\theta}\int_0^{\theta}P_1(s,\tau)d\tau, \tag{10}$$

where

$$\theta=\frac{L}{W}, \tag{11}$$

To simplify the calculations, we transform expression (10) using an asymptotic estimate of the probability integral

$$P_{1s}(s)\approx\frac{\sqrt{4D\theta}}{s^2\sqrt{\pi}}\exp\left(-\frac{s^2}{4D\theta}\right). \tag{12}$$

The full probability of particle drift through the boundary diffusion layer and penetration into the region of the Knudsen layer can be estimated by the formula

$$P_1=\sqrt{\frac{4D\theta}{\pi}}\int_{h_1}^{h}\frac{\exp\left(-\frac{s^2}{4D\theta}\right)}{s^2}ds, \tag{13}$$

The thickness of the Knudsen layer is estimated using the Knudsen number in the form [43]

$$h_1=h\mathrm{Kn}, \tag{14}$$

Since the estimate of the smallness of the diffusion coefficient is correct $D\ll 1$, we obtain an estimate of the integral (13) using the method [42,43]

$$P_1 = \sqrt{\frac{4D\theta}{\pi}}\frac{2D\theta}{h^3}\left[\frac{1}{\mathrm{Kn}^3}\exp\left(-\frac{(\mathrm{Kn}h)^2}{4D\theta}\right)-\exp\left(-\frac{h^2}{4D\theta}\right)\right]. \tag{15}$$

Adjusted for the concentration polarization factor, there is

$$P_1 = \frac{C_1}{C_s}\sqrt{\frac{4D\theta}{\pi}}\frac{2D\theta}{h^3}\left[\frac{1}{\mathrm{Kn}^3}\exp\left(-\frac{(\mathrm{Kn}h)^2}{4D\theta}\right)-\exp\left(-\frac{h^2}{4D\theta}\right)\right], \tag{16}$$

The concentration polarization coefficient will be evaluated according to the recommendations of Karapetyants [44]. Then we get

$$K_p = \frac{C_1}{C_s} \approx \frac{C}{C_1} + \left(1-\frac{C}{C_1}\right)\exp\left(G\frac{h_\mu}{D}\right), \tag{17}$$

where h_μ thickness of the viscous sublayer [37].

Zone II.

To obtain a probabilistic estimate in zone II, consider the geometry of particle motion in the Knudsen layer (Figure 6).

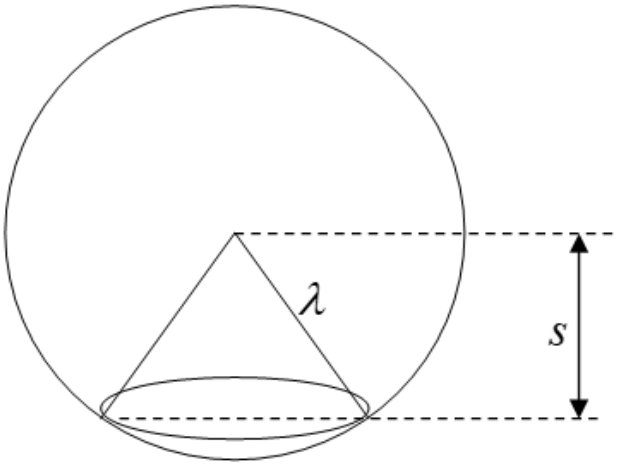

Fig. 6. A diagram of a random walk of particles in the Knudsen layer

Being at a distance not exceeding the free path length from the surface of the membrane, the particle can appear at any point of the ball of radius during the characteristic free path time λ (Figure 6). Therefore, the probability of collision of a particle located at a distance s from the surface of the membrane with the surface can be estimated by the ratio of the volume of the cone with the generate λ and the height s to the volume of the ball with the radius λ

$$P_2(s) = \frac{\lambda - s}{2\lambda}. \tag{18}$$

Integrating the height of the Knudsen layer, we obtain a simple estimate

$$P_2 = \frac{\mathrm{Kn}}{4}. \tag{19}$$

Based on the estimate (19), it is also easy to obtain an expression for the flow of particles of the separated substance in the Knudsen layer.

For the free run length, we use the well-known formula [42]

$$\lambda = \frac{kT}{\pi\sqrt{2}\delta^2(nkT + p)}, \tag{20}$$

Average speed of thermal motion of molecules

$$\overline{V} = \sqrt{\frac{3kT}{m}}, \tag{21}$$

Average residence time in the Knudsen layer [45]

$$\tau = \frac{\sqrt{mkT}}{\pi\sqrt{6}\delta^2\left(nkT + p\right)}. \tag{22}$$

Integrating the thickness of the Knudsen layer using the relations (20), (21), (22), we obtain for the flow of particles to the surface of the membrane in the Knudsen layer

$$j_{\lambda,\tau} = \frac{1}{4\pi\sqrt{2}}\frac{nkT}{\delta^2\left(nkT + p\right)}. \tag{23}$$

Based on an estimate of the Knudsen number

$$\mathrm{Kn} = \frac{\lambda}{h} \tag{24}$$

obtain

$$j_{\lambda,\tau} = \frac{nh}{4}\mathrm{Kn}. \tag{25}$$

Zone III.

The simplest estimate of the probability of penetration into the pore for a particle that has reached the surface of the membrane can be obtained through the specific surface of the pores of

the membrane. For regular cylindrical pores ε_S, this estimate coincides with the porosity of the membrane ε. Taking into account the curvature coefficient of the pores q, we obtain [43]

$$P_3 = \varepsilon_S = \frac{\varepsilon}{q}. \tag{26}$$

Thus, we obtain an estimate of the full probability of particles drifting to the membrane surface from the depth of the solution and their penetration into the pores of the membrane

$$P_S = P_1 P_2 P_3. \tag{27}$$

$$P_S = \frac{\varepsilon}{4q}\mathrm{Kn}\left[\frac{C}{C_1} + \left(1 - \frac{C}{C_1}\exp\left(G\frac{h_\mu}{D}\right)\right)\right]\sqrt{\frac{4D\theta}{\pi}}\frac{2D\theta}{h^3}\times \\ \times\left[\frac{1}{\mathrm{Kn}^3}\exp\left(-\frac{(\mathrm{Kn}h)^2}{4D\theta}\right) - \exp\left(-\frac{h^2}{4D\theta}\right)\right]. \tag{28}$$

The molecular diffusion coefficient present in formula (28) in the vicinity of the membrane differs from the tabular one, since the imperfection of the solution cannot be neglected in this area.

Therefore, we obtain its refined estimate from the following considerations [44].

We use the expression for the chemical potential of the separated substance from the theory of dilute solutions

$$\nu = \nu^* + RT\ln C + \omega_{AX}(1-C)^2, \tag{29}$$

To correct for imperfection, the ratio can be used [44]

$$\omega_{AX} = \kappa\left[2\varepsilon_{AX} - \varepsilon_{XX}\right] \tag{30}$$

Since the solution is taken diluted, we assume that $C \ll 1$ and the interaction between the molecules *A* and *A* can be neglected.

Then we can write an approximate equality

$$\nu = \nu^* + RT\ln C + \omega_{AX}(1-2C). \tag{31}$$

In accordance with the provisions of the thermodynamics of dilute solutions, the diffusion coefficient is determined by the value of the derivative of the chemical potential in concentration [44]. Then we get

$$\frac{\partial\nu}{\partial C} = \frac{RT}{C} - 2\omega_{AX} = \frac{RT}{C}(1 - 2\omega_{AX}C). \tag{32}$$

Hence follows

$$D = D_i(1 - 2\omega_{AX}C), \tag{33}$$

As noted by Smirnov and Bartov [42], estimating the probability of particles passing through the pore is currently too difficult a task, for which no sufficiently substantiated recommendations have yet been developed. The estimates given in the study by Smirnov and Bartov [42] can be used. At the same time, knowledge of the fine structure of the adsorption layer inside the pore is required, which is hardly available in engineering calculations. However, in our opinion, in the case of ultrafiltration, the tunneling effect can be neglected, which manifests itself only at the quantum mechanical level. Indeed, overcoming the potential barrier occurs as a result of internal autocatalysis, i.e., the socialization of external quantum electronic levels with a decrease in the energy barrier.

Lightweight transfer membranes represent a promising group of membranes for achieving high ion separation accuracy, especially ions with similar sizes and charges [46]. Gelation is an effective means of improving membrane performance by balancing the mobility of transport carriers and stability in the membrane. This work serves as a demonstration of the creation of highly efficient selective membranes with facilitated transfer by gelation. According to Satayev *et al.,* [47], a mathematical simulation of the ultrafiltration of a solution of the polymer methoxyanabazine $C_{11}H_{16}N_2O$ was developed. The study by Aguiar *et al.,* [48] is devoted to thin-film composite ultrafiltration membranes in which the selective layers consist of zwitterion-containing hydrogels, which leads to increased permeability, selectivity and resistance to contamination. In the study by Lazarev *et al.,* [49], a mathematical description of the formation of a sediment layer on the membrane surface due to concentration polarization was performed based on a semi-integral method for solving the convective diffusion equation, optimizing the ultrafiltration process and determining the sediment layer on the membrane surface, as well as calculating the operating time of the membrane and the volume of filtrate in steady state before regeneration.

Then only the summand can be preserved in the Arrhenius-Gamow formula. describing the effect of activation energy E_{act} for solvent passage

$$P_{IV} \approx A\exp\left(-\frac{E_{act}}{kT}\right), \tag{34}$$

To estimate the frequency factor, we use the ratio of the interparticle distance in the pore to the free path length. Since in the solvent flow outside the membrane, the interparticle distance is estimated by the formula

$$l_e \approx \sqrt[3]{1/C_1}\,, \tag{35}$$

then inside the pore the appropriate estimate should take into account the free volume of the flow

$$l_i \approx \sqrt[3]{1/(\varepsilon C_1)}\,. \tag{36}$$

Hence follows

$$P_{IV} \approx \frac{\sqrt[3]{1/(\varepsilon C_1)}}{\lambda}\exp\left(-\frac{E_{act}}{kT}\right). \tag{37}$$

Now the theoretical assessment of membrane selectivity can be written as

$$\varphi = P_S P_{IV} . \tag{38}$$

To fully verify the adequacy of this model, it is necessary to compare it with a large amount of experimental data. Then it will be possible to refine some estimates using correction coefficients. Figure 7 shows some results of numerical experiments for the following values of the model parameters

$\mathrm{Kn} \propto 10^{-4}$; $h \propto 10^{-3} \div 10^{-2}$ м; $h_\mu \propto 10^{-5} \div 10^{-6}$; $D \propto 10^{-9}$ м²/s;
$\omega_{AX} \propto 0{,}01 \div 0{,}05$ $C_1 \propto 5 \div 20$ mol/м³ ; $G \approx 10^{-2}$ м/s; $\varepsilon \propto 0{,}02 \div 0{,}2$; $q \propto 1{,}5$;
$\theta \propto 10$ s.

The calculation results are generally in qualitative agreement with the known patterns of ultrafiltration and experimental data [46-49].

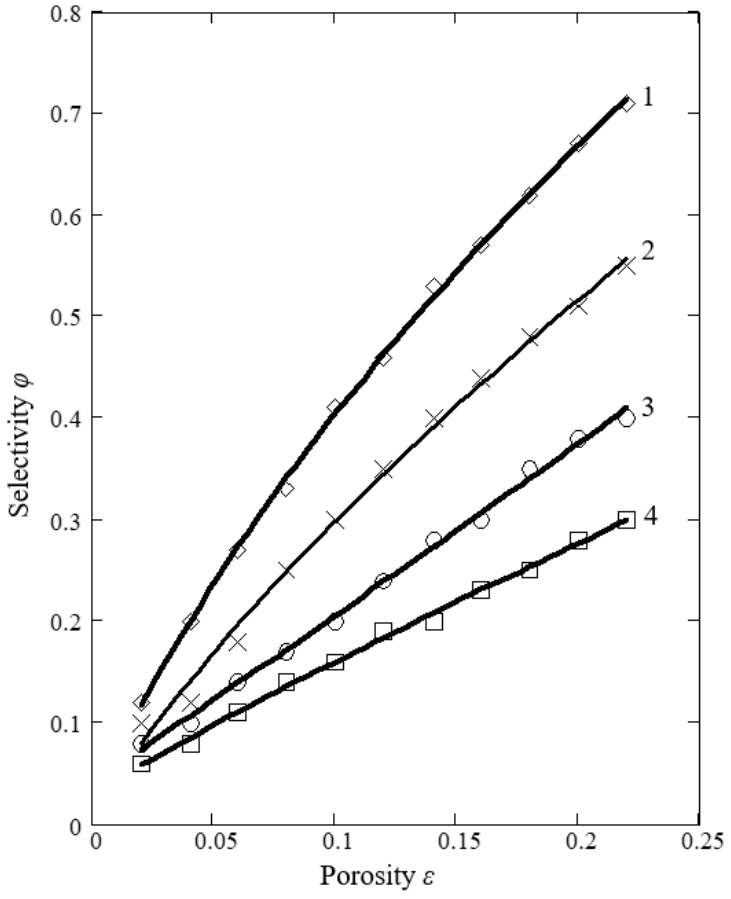

Fig. 7. Characteristic curves of a numerical experiment based on a probabilistic selectivity model. Dependence of selectivity on porosity. 1 - $C_1 = 5$ mol/m³; 2 - $C_1 = 3$ mol/m³; 3 - $C_1 = 10$ mol/m³; 4 - $C_1 = 16$ mol/m³

3.2 Modeling of the Dissolution of an Impurity in a Membrane Pore in a Medium with Surface-Active Micelles

Surfactants are used in membrane technologies to create an environment that promotes accelerated dissolution of droplets of substances with low solubility penetrating into the membrane pores. This method is used in soil purification from organic solvents, separation of water-organic impurities, in oil production, pharmaceutical industry, etc. [44,45].

Surfactants, as a rule, form local formations in the solvent - micelles. Micelles capture both partially dissolved impurity molecules directly from the solution and adsorb small droplets of the insoluble part of the impurity in the medium.

It is established that, in general, the solubilization process occurs in several stages and its full description today seems difficult.

In this paper, a simplified model of the process of dissolving an impurity drop in a membrane pore is proposed, taking into account the presence of surfactant micelles in the solution.

At the same time, we believe that the solubilization process occurs mainly by the reaction-diffusion mechanism, i.e. the molecules of the solute diffuse to the surface of the micelle and enter into a solubilization reaction on its surface.

The corresponding mathematical model of this process looks as follows [45]

$$\frac{\partial a}{\partial t} = k_a C_m C, \tag{39}$$

According to the accepted diffusion-reaction mechanism of dissolution, it is possible to write down the diffusion equation of an impurity substance in a membrane pore, taking into account solubilization

$$\frac{\partial C}{\partial t} + \frac{\partial a}{\partial t} = D\frac{\partial^2 C}{\partial z^2}, \tag{40}$$

Taking into account the ratio (39), we obtain the following reaction-diffusion equation for the solubilization of a drop in a pore membrane

$$\frac{\partial C}{\partial t} = D\frac{\partial^2 C}{\partial z^2} - k_a C_m C, \tag{41}$$

where z - longitudinal coordinate (along the pore axis – Figure 8).

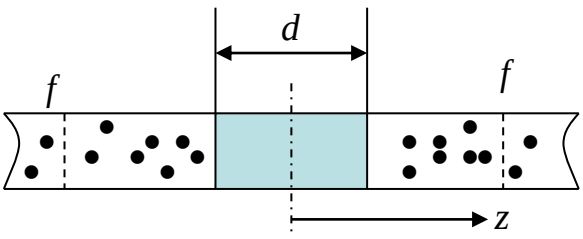

Fig. 8. Diagram of the solubilization process in a pore membrane

The boundary conditions are as follows

$$C\left(\frac{d}{2},t\right)=C_{eq}, \tag{42}$$

$$a\left(\frac{d}{2},t\right)=0, \tag{43}$$

If we introduce the idea of the micellar capture front, i.e. the distance f from the droplet in the vapor, which is affected by the impurity in the membrane pore, then the boundary conditions can be supplemented by the relations [50,51]

$$C\left(f,t\right)=0, \tag{44}$$

$$a\left(f,t\right)=0\ . \tag{45}$$

Eq. (41), provided that the concentration of micelles in the solution is constant, has a traveling wave type solution.

Indeed, we introduce a self-similar variable

$$\eta=z+wt, \tag{46}$$

Then, Eq. (41) is transformed to the form

$$w\frac{dC}{d\eta}=D\frac{d^2C}{d\eta^2}-k_aC_mC\cdot \tag{47}$$

The general solution of this equation has the form

$$C=C_1\exp\left(\lambda_1\eta\right)+C_2\exp\left(\lambda_2\eta\right), \tag{48}$$

where

$$\lambda_{1,2}=\frac{w\pm\sqrt{w^2+4Dk_aC_m}}{2D}. \tag{49}$$

From the limitation condition of the solution, we obtain

$$C=C_{eq}\exp\left[\frac{w-\sqrt{w^2+4Dk_aC_m}}{2D}\left(z+wt\right)\right]\cdot \tag{50}$$

Introduce the notation

$$\lambda = \frac{w - \sqrt{w^2 + 4Dk_a C_m}}{2D}. \tag{51}$$

From the balance ratios, it is possible to obtain a relationship between the time of complete dissolution of the drop τ and the length of the dissolution trace f.

Indeed, the mass of the dissolved substance, taking into account the micellar capture in the dissolution trace, is equal to

$$M = S \int_0^{f - w\tau} C d\eta, \tag{52}$$

On the other hand, this mass is equal to the mass of the dissolved drop

$$M = \rho d S, \tag{53}$$

So, we get:

$$C_{eq}\left(\exp(\lambda(f + w\tau) - 1\right) = \rho\lambda d. \tag{54}$$

Taking a certain average value as the velocity of the dissolution front, we obtain

$$\overline{w} = \frac{f}{\tau}. \tag{55}$$

$$C_{eq}\left(\exp(2\lambda f) - 1\right) = \rho\lambda d. \tag{56}$$

From here we get an estimate of the length of the dissolution front

$$f \approx \frac{1}{2\lambda} \ln\left(\frac{\rho\lambda d}{M C_{eq}} + 1\right), \tag{57}$$

An estimate of the average velocity of the dissolution front can be obtained from the following considerations. β - the mass transfer coefficient along the interfacial surface of the drop-micellar solution.

Then Fick's law is valid for the flow of a dissolving substance j

$$j = -D \left.\frac{\partial C}{\partial z}\right|_{z=\frac{d}{2}} \approx -\beta C_{eq}. \tag{58}$$

Thus, we obtain a formula for calculating the length of the dissolution front in a micellar solution inside a membrane pore – the ratio (57), where: $\overline{w}$

$$\overline{w} \approx \beta . \tag{59}$$

Thus, we obtain a formula for calculating the length of the dissolution front in a micellar solution inside a membrane pore – the ratio (57), where

$$\lambda = \frac{\beta - \sqrt{\beta^2 + 4Dk_a C_m}}{2D} . \tag{60}$$

In the study by Rho *et al.,* [52], it was found that the decrease in diffusion coefficients was noticeably pronounced when membranes rich in ionizable functional groups with strong negative charges were used, indicating increased electrostatic repulsion. The aim of the study by Momeni *et al.,* [53] was to investigate momentum, heat and mass transfer using 3D CFD modeling for a module with a hollow fiber membrane. The three-dimensional equations of momentum, heat transfer and mass transfer were combined and solved using the finite volume method using the Comsol Multiphase software. Computational fluid dynamics modeling was performed to obtain high-precision data on the hydrodynamics and mass transfer behavior of membrane channels filled with separators [54]. Modeling was used to study the effect of geometric parameters of gaskets on pressure loss and concentration polarization in membrane channels. In a study by Yang *et al.,* [55], overcoming the limitation of mass transfer caused by agglomeration of the catalyst powder was studied. Powder catalysts based on perovskite were embedded in a polyacrylonitrile ultrafiltration membrane with phase transformation. Hollow fiber membrane contactors are a promising technology for the removal and recovery of ammonia from liquid wastewater [56]. However, a better understanding is required.

Figure 9 shows the dependence of the parameter λ from the mass transfer coefficient along the interface β, and in Figure 10, the dependence of the wavefront length on the coefficient β.

The numerical experiment was carried out at the following parameter values

$$\beta = 10^{-3} \div 2 \cdot 10^{-2}\, м/с;\ D \sim 10^{-6}\, м^2/с;\ k_a C_m \sim 10\ \frac{1}{с};\ d \sim 10^{-3}\, м$$

The calculation results are generally in qualitative agreement with the known patterns of ultrafiltration and experimental data [52-56].

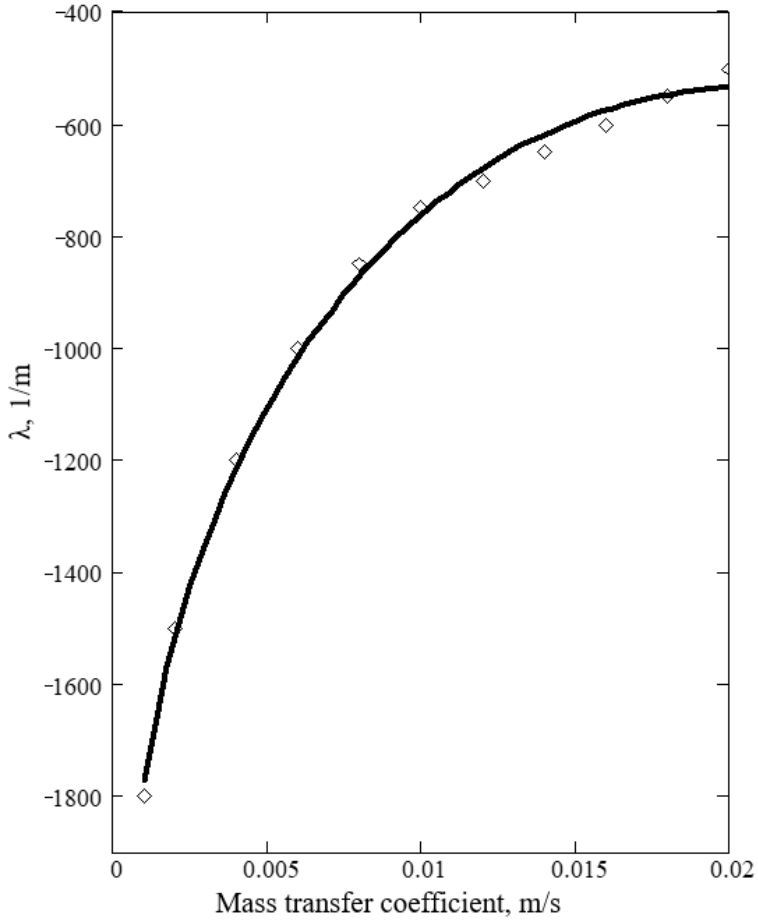

Fig. 9. Dependence of the parameter on the mass transfer coefficient

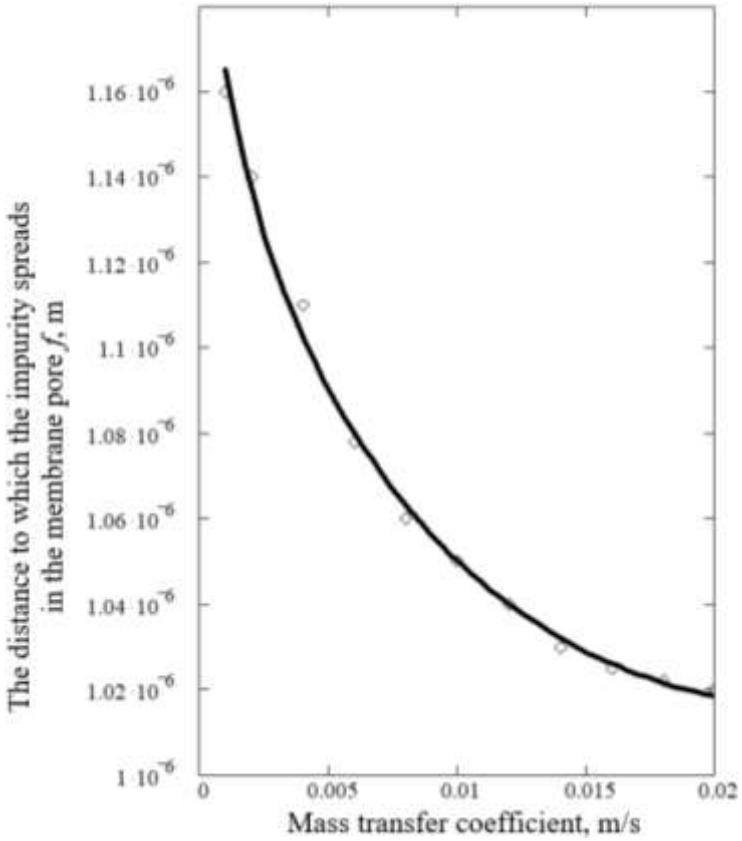

Fig. 10. Dependence of the wavefront length on the mass transfer coefficient

4. Conclusions

A probabilistic approach was used to theoretically evaluate the selectivity of ultrafiltration membranes, in which the mechanism of the separation process differs significantly from the mechanism of separation in nanomembranes. Adjusted for the concentration polarization factor, an equation is obtained for calculating the total probability of particle drift through the boundary diffusion layer and penetration into the region of the Knudsen layer.

Integrating the thickness of the Knudsen layer using the ratios for calculating the free path of molecules, the average speed of thermal motion of molecules, the average residence time in the Knudsen layer, an equation is obtained for calculating the flow of particles to the membrane surface in the Knudsen layer.

An estimate of the total probability of particles drifting to the membrane surface from the depth of the solution and their penetration into the pores of the membrane is obtained, taking into account the molecular diffusion coefficient in the vicinity of the membrane, which differs from the tabular one, since the imperfection of the solution cannot be neglected in this area.

An equation is obtained for calculating the diffusion coefficient taking into account the molecular diffusion coefficient in an ideal system, as well as equations for calculating permeability in pores, taking into account the influence of the activation energy for the passage of the solvent.

A theoretical assessment of membrane selectivity is given based on the full probability of particles drifting to the membrane surface from the depth of the solution and their penetration into the pores of the membrane. The characteristic curves of the numerical experiment based on the probabilistic selectivity model and the dependence of selectivity on porosity are determined.

A formula has been obtained for calculating the length of the dissolution front in a micellar solution inside a membrane pore, taking into account the diffusion and mass transfer coefficients.

Acknowledgement
This research was funded by Ministry of Science and Higher Education of the Republic of Kazakhstan grant number AP19678142 “Development of drying equipment and mass transfer research for fruit drying.”

References

[1] Guo, Yongqiang, Hongbin Li, and Chao Liu. "Confined mass transfer mechanism and preparation strategies of separation membranes: A review." *Materials & Design* 227 (2023): 111805. https://doi.org/10.1016/j.matdes.2023.111805

[2] Ahmad, Fatin Nurwahdah, Norazlianie Sazali, Safwan Shalbi, Nor Hasrul Akhmal Ngadiman, and Mohd Hafiz Dzarfan Othman. "Oxygen separation process using ceramic-based membrane: A review." *Journal of Advanced Research in Fluid Mechanics and Thermal Sciences* 62, no. 1 (2019): 1-9.

[3] Kumar, Bavanasi Pradeep, and Sangapatnam Suneetha. "Numerical Investigation of Diffusion Thermo and Thermal Diffusion on MHD Convective Flow of Williamson Nanofluid on a Stretching Surface Through a Porous Medium in the Presence Chemical Reaction and Thermal Radiation." *Journal of Advanced Research in Fluid Mechanics and Thermal Sciences* 115, no. 2 (2024): 141-157. https://doi.org/10.37934/arfmts.115.2.141157

[4] Ghazali, Nazlee Faisal, and Ki Min Lim. "Mass transport models in organic solvent nanofiltration: a review." *Journal of Advanced Research in Fluid Mechanics and Thermal Sciences* 76, no. 3 (2020): 126-138. https://doi.org/10.37934/arfmts.76.3.126138

[5] Abubakar, Muazu, and Norhayati Ahmad. "Preparation and Characterization of a Clay-Based Ceramic Membrane for Tannery Wastewater Treatment." *Journal of Advanced Research in Applied Sciences and Engineering Technology* 30, no. 1 (2023): 1-14. https://doi.org/10.37934/araset.30.1.114

[6] Mokhtar, Hamizah, Afizah Ayob, Duratul Ain Tholibon, and Zulhafizal Othman. "Preparation and characterization of polysulfone composite membrane blended with kenaf cellulose fibrils." *Journal of Advanced Research in Applied Sciences and Engineering Technology* 31, no. 2 (2023): 91-100. https://doi.org/10.37934/araset.31.2.91100

[7] Ghani, Nik Rashida Nik Abdul, and Mohammed Saedi Jami. "Dynamic Adsorption of Lead by Novel Graphene Oxide-polyethersulfone Nanocomposite Membrane in Fixed-bed Column." *Journal of Advanced Research in Experimental Fluid Mechanics and Heat Transfer* 2, no. 1 (2020): 1-9.

[8] Lounder, Samuel J., Patrick T. Wright, Luca Mazzaferro, and Ayse Asatekin. "Fouling-resistant membranes with tunable pore size fabricated using cross-linkable copolymers with high zwitterion content." *Journal of Membrane Science Letters* 2, no. 1 (2022): 100019. https://doi.org/10.1016/j.memlet.2022.100019

[9] Ghouri, Zafar Khan, Khaled Elsaid, David James Hughes, Mohamed Mahmoud Nasef, Ahmed Abdel-Wahab, and Ahmed Abdala. "Strong improvement of permeability and rejection performance of graphene oxide membrane by engineered interlayer spacing." *Journal of Membrane Science Letters* 3, no. 2 (2023): 100065. https://doi.org/10.1016/j.memlet.2023.100065

[10] Habib, Shahriar, Bryn E. Larson, and Steven T. Weinman. "Effect of surfactant structure on MPD diffusion for interfacial polymerization." *Journal of Membrane Science Letters* 3, no. 2 (2023): 100055. https://doi.org/10.1016/j.memlet.2023.100055

[11] Satayev, Marat, Omirbek Baiysbay, Abdugani Azimov, Nina Alekseyeva, Saule Khamzayeva, and Sherkhan Yergalyuly. "Modelling the dependence of the internal diffusion coefficient and hydrodynamic resistance on the structures and shapes of polymer membrane pores." *Heat and Mass Transfer* 58, no. 2 (2022): 295-308. https://doi.org/10.1007/s00231-021-03103-z

[12] Luo, Xinzhao, Xin Liu, Yaqi Dong, Liyuan Fan, Tianheng Wang, and Qiang Zhang. "Dehydration-induced stable boroxine network as selective layer of anti-dye-deposition membranes." *Journal of Membrane Science* 687 (2023): 122082. https://doi.org/10.1016/j.memsci.2023.122082

[13] Gowda, Dwani Venkataswamy, Danny Harmsen, Arnout D'Haese, and Emile R. Cornelissen. "Membrane integrity monitoring on laboratory scale: Impact of test cell-induced damage on membrane selectivity." *Journal of Membrane Science* 669 (2023): 121281. https://doi.org/10.1016/j.memsci.2022.121281

[14] Blatt, William F., Arun Dravid, Alan S. Michaels, and Lita Nelsen. "Solute polarization and cake formation in membrane ultrafiltration: causes, consequences, and control techniques." In *Membrane Science and Technology: Industrial, Biological, and Waste Treatment Processes*, pp. 47-97. Boston, MA: Springer US, 1970. https://doi.org/10.1007/978-1-4684-1851-4_4

[15] Doshi, Mahendra R. "Boundary layer removal in ultrafiltration." In *Ultrafiltration Membranes and Applications*, pp. 231-246. Boston, MA: Springer US, 1980. https://doi.org/10.1007/978-1-4613-3162-9_15
[16] Raff, Manfred. "Mass Transfer Models Across Membranes." In *Mass Transfer Models in Membrane Processes: Applications in Artificial Organs*, pp. 13-32. Cham: Springer International Publishing, 2021. https://doi.org/10.1007/978-3-030-89195-4_3
[17] Espinoza-Gómez, Heriberto, Shui Wai Lin, and Eduardo Rogel-Hernández. "Determination of pore diameter from rejection measurements with a mixture of oligosaccharides." *Heat and Mass Transfer* 41 (2005): 503-509. https://doi.org/10.1007/s00231-004-0573-x
[18] Aimar, Pierre, Martine Meireles, Patrice Bacchin, and Victor Sanchez. "Fouling and concentration polarisation in ultrafiltration and microfiltration." *Membrane Processes in Separation and Purification* (1994): 27-57. https://doi.org/10.1007/978-94-015-8340-4_3
[19] Fedosov, S. V., Yu P. Osadchy, and A. V. Markelov. "Modeling of ultrafiltration process taking into account the formation of sediment on membrane surface." *Membranes and Membrane Technologies* 2 (2020): 169-180. https://doi.org/10.1134/S251775162003004X
[20] Mulder, Marcel, and Marcel Mulder. "Polarisation phenomena and membrane fouling." *Basic Principles of Membrane Technology* (1996): 416-464. https://doi.org/10.1007/978-94-009-1766-8_7
[21] Caravella, Alessio. "Concentration polarization coefficient (CPC)." *Encyclopedia of Membranes* (2016): 440-441. https://doi.org/10.1007/978-3-662-44324-8_1642
[22] Bryll, Arkadiusz, and Andrzej Ślęzak. "The mathematical model of concentration polarization coefficient in membrane transport and volume flows." *Journal of Biological Physics* 43 (2017): 31-44. https://doi.org/10.1007/s10867-016-9432-5
[23] Dmitriev, E. A., and I. K. Kuznetsova. "Analysis of the applicability of the electrodiffusion method to the modeling of external mass transfer during reverse osmosis and ultrafiltration." *Theoretical Foundations of Chemical Engineering* 35, no. 2 (2001): 124-128. https://doi.org/10.1023/A:1010321304893
[24] Polyakov, Yu S. "Pore constriction in ultrafiltration: a discrete multilayer deposition model with steric exclusion of solutes at the pore inlet." *Theoretical Foundations of Chemical Engineering* 48 (2014): 382-396. https://doi.org/10.1134/S004057951404023X
[25] Yi, Xuesong, Jiahui Li, Dexin Wang, Yong Wang, Shuo Wang, and Fei Yang. "The underlying mechanism in gel formation and its mathematical simulation during anionic polyacrylamide solution ultrafiltration process." *Environmental Science and Pollution Research* 27 (2020): 27124-27134. https://doi.org/10.1007/s11356-020-09084-6
[26] Baikov, V. I., and A. V. Bil'Dyukevich. "Nonstationary concentration polarization in laminar ultrafiltration in a plane channel." *Journal of Engineering Physics and Thermophysics* 67, no. 1 (1994): 773-776. https://doi.org/10.1007/BF00853332
[27] Sherwood, Thomas Kilgore, Robert Lamar Pigford, and Charles R. Wilke. *Mass transfer*. New York: McGraw-Hill, 1982.
[28] Pandey, Ras B., Kelly L. Anderson, and Barry L. Farmer. "Effect of temperature and solvent on the structure and transport of a tethered membrane: Monte Carlo simulation." *Journal of Polymer Science Part B: Polymer Physics* 43, no. 23 (2005): 3478-3486. https://doi.org/10.1002/polb.20642
[29] Liu, Q., S. Xiao, D. De Kee, and C. Moresoli. "Diffusion in elongated membranes." *Journal of Applied Polymer Science* 99, no. 5 (2006): 2746-2751. https://doi.org/10.1002/app.22965
[30] Mohammadi, Toraj, Aliasghar Kohpeyma, and Mohtada Sadrzadeh. "Mathematical modeling of flux decline in ultrafiltration." *Desalination* 184, no. 1-3 (2005): 367-375. https://doi.org/10.1016/j.desal.2005.02.060
[31] Vlachos, D. G., and M. A. Katsoulakis. "Derivation and validation of mesoscopic theories for diffusion of interacting molecules." *Physical Review Letters* 85, no. 18 (2000): 3898. https://doi.org/10.1103/PhysRevLett.85.3898
[32] Snyder, M. A., D. G. Vlachos, and M. A. Katsoulakis. "Mesoscopic modeling of transport and reaction in microporous crystalline membranes." *Chemical Engineering Science* 58, no. 3-6 (2003): 895-901. https://doi.org/10.1016/S0009-2509(02)00621-8
[33] Horntrop, David J., Markos A. Katsoulakis, and Dionisios G. Vlachos. "Spectral methods for mesoscopic models of pattern formation." *Journal of Computational Physics* 173, no. 1 (2001): 364-390. https://doi.org/10.1006/jcph.2001.6883
[34] Geraldes, Vítor, and Maria Norberta De Pinho. "Mass transfer coefficient determination method for high-recovery pressure-driven membrane modules." *Desalination* 195, no. 1-3 (2006): 69-77. https://doi.org/10.1016/j.desal.2005.10.035
[35] Cherevko, K. V., D. A. Gavryushenko, and V. M. Sysoev. "The influence of the chemical reactions on the diffusion phenomena in the cylincrical systems bounded with the membranes." *Journal of Molecular Liquids* 127, no. 1-3 (2006): 71-72. https://doi.org/10.1016/j.molliq.2006.03.018

[36] Puri, P., J. Hinestroza, and D. De Kee. "Transport of small molecules through mechanically elongated polymeric membranes." *Journal of Applied Polymer Science* 96, no. 4 (2005): 1200-1203. https://doi.org/10.1002/app.21375
[37] Dytnersky, Yuri Iosifovich. "Reverse osmosis and ultrafiltration." *Chemistry* (1978): 351.
[38] Dytnersky, Yuri Iosifovich. " Baromembrane processes." *Chemistry* (1986): 272.
[39] Jerayan, T. G., Shkinev, V. M., Danilova, T. V., and Karandashev, V. K. "Multistage membrane systems for continuous fractionation of waters in analysis." *Membranes* 9 (2001): 34-37.
[40] Skobeev, Ivan Konstantinovich. "Filter materials." *Nedra* (1978): 200.
[41] Satayev, Marat Isakovich. "Ensuring environmental safety of the environment using adsorption and membrane methods for purifying water and gas flows." *PhD diss., Auezov South Kazakhstan State University, Shymkent* (2006).
[42] Smirnov, A. V., and A. S. Bartov. "Probabilistic approach in assessing membrane selectivity for individual ions." *Membranes* 26 (2005): 23-30.
[43] Nakagaki, M. "Physical chemistry of membranes." *Mir* (1991): 254.
[44] Karapetyants, M. Kh. "Chemical thermodynamics." *Chemistry* (1975): 584.
[45] Falbe, Jürgen, ed. *Surfactants in consumer products: Theory, Technology and Application*. Springer Science & Business Media, 1986.
[46] Yang, Yanshao, Yuzhang Zhu, Youjing Zhao, Zejun Song, Di Zhu, Min Wang, Jian Jin, and Wangxi Fang. "Gelation induced selectivity enhancement of facilitated transport membranes and its relation to ion transport resistance." *Journal of Membrane Science* 701 (2024): 122757. https://doi.org/10.1016/j.memsci.2024.122757
[47] Satayev, Marat, Birzhan Shakirov, Botagoz Mutaliyeva, Lazzat Satayeva, Rustem Altynbekov, Omirbek Baiysbay, and Ravshanbek Alibekov. "Mathematical modeling of methoxyanabasine $C_{11}H_{16}N_2O$ polymer solution ultrafiltration." *Heat and Mass Transfer* 48 (2012): 979-987. https://doi.org/10.1007/s00231-011-0948-8
[48] Aguiar, Alice Oliveira, Hyunmin Yi, and Ayse Asatekin. "Fouling-resistant membranes with zwitterion-containing ultra-thin hydrogel selective layers." *Journal of Membrane Science* 669 (2023): 121253. https://doi.org/10.1016/j.memsci.2022.121253
[49] Lazarev, S. I., O. A. Abonosimov, S. I. Kotenev, and K. V. Shestakov. "Theoretical calculation of concentration polarization in the ultrafiltration purification of technological solutions containing trisodium phosphate." *Theoretical Foundations of Chemical Engineering* 56, no. 6 (2022): 1015-1019. https://doi.org/10.1134/S0040579522060094
[50] Threatov, V. V., and A. N. Filippov. "Accelerated dissolution of a drop of impurity liquid in a membrane pore (capillary) filled with a micellar solution." *Membranes* 3 (2004): 23.
[51] Adamson, Arthur W., and Alice Petry Gast. *Physical chemistry of surfaces*. Wiley, 1997.
[52] Rho, Hojung, Byung-Moon Jun, Yun Chul Woo, Chanhyuk Park, Kangmin Chon, and Jaeweon Cho. "Evaluation of diffusion coefficients as surrogate indicators for electrostatic repulsion in ultrafiltration membrane fouling." *Desalination* 568 (2023): 117020. https://doi.org/10.1016/j.desal.2023.117020
[53] Momeni, Mohammadreza, Ali Kargari, Mitra Dadvar, and Arezoo Jafari. "3D-CFD simulation of hollow fiber direct contact membrane distillation module: Effect of module and fibers geometries on hydrodynamics, mass, and heat transfer." *Desalination* 576 (2024): 117321. https://doi.org/10.1016/j.desal.2024.117321
[54] Binger, Zachary M., and Andrea Achilli. "Surrogate modeling of pressure loss & mass transfer in membrane channels via coupling of computational fluid dynamics and machine learning." *Desalination* 548 (2023): 116241. https://doi.org/10.1016/j.desal.2022.116241
[55] Yang, Na, Jingchao Yu, Longfei Zhang, Yongli Sun, Luhong Zhang, and Bin Jiang. "Integration of efficient $LaSrCoO_4$ perovskite and polyacrylonitrile membrane to enhance mass transfer for rapid contaminant degradation." *Journal of Water Process Engineering* 53 (2023): 103804. https://doi.org/10.1016/j.jwpe.2023.103804
[56] Aguilar-Moreno, Miguel, J. Lopez, Elena Guillen-Burrieza, M. Reig, C. Valderrama, and J. L. Cortina. "Ammonium recovery and concentration from synthetic wastewater using a poly (4-methyl-1-pentene)(PMP) liquid-liquid membrane contactor: Flux performance and mass transport characterization." *Separation and Purification Technology* 326 (2023): 124657. https://doi.org/10.1016/j.seppur.2023.124657